INFECTION AND IMMUNITY, Aug. 2007, p. 3758–3768 Vol. 75, No. 8
0019-9567/07/$08.00+0 doi:10.1128/IAI.00225-07

Plasmodium yoelii Sporozoites with Simultaneous Deletion of P52 and P36 Are Completely Attenuated and Confer Sterile Immunity against Infection▽

Mehdi Labaied,[1] Anke Harupa,[1] Ronald F. Dumpit,[1] Isabelle Coppens,[2] Sebastian A. Mikolajczak,[1] and Stefan H. I. Kappe[1,3]*

Seattle Biomedical Research Institute, Seattle, Washington 98109[1]; Department of Molecular Microbiology and Immunology and The Malaria Research Institute, Johns Hopkins University Bloomberg School of Public Health, Baltimore, Maryland 21205[2]; and Department of Pathobiology, University of Washington, Seattle, Washington 98195[3]

Received 11 February 2007/Returned for modification 18 March 2007/Accepted 9 May 2007

Malaria infection starts when sporozoites are transmitted to the mammalian host during a mosquito bite. Sporozoites enter the blood circulation, reach the liver, and infect hepatocytes. The formation of a parasitophorous vacuole (PV) establishes their intracellular niche. Recently, two members of the 6-Cys domain protein family, P52 and P36, were each shown to play an important albeit nonessential role in *Plasmodium berghei* sporozoite infectivity for the rodent host. Here, we generated *p52*/*p36*-deficient *Plasmodium yoelii* parasites by the simultaneous deletion of both genes using a single genetic manipulation. *p52*/*p36*-deficient parasites exhibited normal progression through the life cycle during blood-stage infection, transmission to mosquitoes, mosquito-stage development, and sporozoite infection of the salivary glands. *p52*/*p36*-deficient sporozoites also showed normal motility and cell traversal activity. However, immunofluorescence analysis and electron microscopic observations revealed that *p52*/*p36*-deficient parasites did not form a PV within hepatocytes in vitro and in vivo. The *p52*/*p36*-deficient parasites localized as free entities in the host cell cytoplasm or the host cell nucleoplasm and did not develop as liver stages. Consequently, they did not cause blood-stage infections even at high sporozoite inoculation doses. Mice immunized with *p52*/*p36*-deficient sporozoites were completely protected against infectious sporozoite challenge. Our results demonstrate for the first time the generation of two-locus gene deletion-attenuated parasites that infect the liver but do not progress to blood-stage infection. The study will critically guide the design of *Plasmodium falciparum* live attenuated malaria vaccines.

Plasmodium parasites have multiple and distinct stages that constitute their complex life cycle in the mosquito vector and mammalian host. The parasite's invasive stages actively infect cells of the mammalian host, wherein replication occurs to produce the next generation of infectious forms. Invasive sporozoites that are transmitted by the bite of a female *Anopheles* mosquito infect hepatocytes and initiate the liver-stage (LS) phase, which grows and leads to the development of red blood cell-infectious merozoites (19, 24). Because malaria pathology is associated exclusively with blood-stage infection, a vaccine that efficiently targets the sporozoite and/or LS could completely prevent the onset of disease.

Once deposited into the host skin by a mosquito bite, the motile sporozoites actively enter blood vessels and are transported by the blood circulation to the liver (34). In the liver, they cross the vascular endothelium by passage through resident Kupffer cells in order to reach the space of Disse (1, 6). This allows them free access to hepatocytes (11). Sporozoites traverse several hepatocytes (5, 20) before they infect a single hepatocyte by forming a replication-permissive parasitophorous vacuole (PV) compartment. The molecular mechanisms that control the parasites' complex journey and the final establishment of an intrahepatocytic niche are poorly understood, but a number of sporozoite proteins on the cell surface or in the secretory organelles have emerged as being critical for distinct steps (14). The best-studied proteins are the circumsporozoite protein (CSP) and the thrombospondin-related anonymous protein (TRAP). CSP and TRAP are involved in various steps of mammalian host infection such as gliding motility, host cell recognition, and host cell invasion. Parasites lacking CSP do not form sporozoites within oocysts (18), and parasites lacking TRAP completely lose the ability to infect the mosquito salivary glands and hepatocytes (29). More recently, sporozoite microneme protein essential for cell traversal 1 (SPECT1) (11), the *Plasmodium* perforin-like protein 1 (PPLP1) (9, 12), and the cell traversal protein for ookinete and sporozoite activity (CelTOS) (16) were specifically implicated in cell traversal. However, parasites with a targeted disruption of the genes encoding cell traversal-associated proteins retain their ability to infect and grow in hepatocytes. Recently, two additional proteins, P52 (also termed P36p) (15) and P36 (31), have been implicated in sporozoite infection of hepatocytes by *Plasmodium berghei* but not gliding motility or cell traversal (10, 35). P52 and P36 are members of the 6-Cys protein superfamily characterized by domains with six position-conserved cysteines, a structure unique to *Plasmodium* species (3). Eight genes from this family are arranged as paralogous gene

* Corresponding author. Mailing address: Seattle Biomedical Research Institute, 307 Westlake Avenue North, Suite 500, Seattle, WA 98109-5219. Phone: (206) 256-7205. Fax: (206) 256-7229. E-mail: stefan.kappe@sbri.org.

▽ Published ahead of print on 21 May 2007.

pairs. The P52 and P36 genes are arranged in tandem in the genome of *Plasmodium yoelii* (contig MALPY00354) and other *Plasmodium* species. Different members of the 6-Cys superfamily are expressed in distinct parasite stages. The gametocyte-expressed members P48 and P45 are critical for gamete fertilization, and P230 is important for the interaction of male gametes with red blood cells (4, 36). Thus, 6-Cys proteins are likely parasite ligands that mediate interactions between gametes or the interaction of parasites and host cells. Interestingly, a recent structure prediction analysis showed similarity between 6-Cys proteins and *Toxoplasma gondii* SAG1 (surface antigen 1), a member of the glycosylphosphatidylinositol (GPI)-linked surface proteins, which mediates attachment to host cells (7). P52 and P36 are uniquely expressed in sporozoites. A lack of P52 that localized to the secretory micronemes shows a significant but not complete reduction of infectivity for the mammalian host (10, 35). Those two studies showed conflicting results concerning the phenotype of *p52*-deficient parasites. Ishino et al. (10) found that *p52*-deficient parasites significantly increased their cell traversal activity and could form a PV upon invasion. In contrast, van Dijk et al. (35) did not observe an increase in cell traversal and did not observe a PV late in infection. We have shown that UIS3 and UIS4 (upregulated in infective sporozoite genes 3 and 4), small membrane proteins of the sporozoite secretory organelles (13), and the LS PV membrane (PVM) are essential for LS development of *P. berghei* (21, 22). *P. yoelii uis3*- and *uis4*-deficient sporozoites successfully invade host cells and form the early LS inside an intact PV, but they fail to develop and in consequence cannot initiate blood-stage infection (30). Strikingly, parasites that infect the liver but are unable to undergo growth make powerful vaccines. Immunizations with *uis3*- or *uis4*-deficient sporozoites completely protected mice against subsequent infectious sporozoite challenge (21, 22). The use of genetically attenuated parasites (GAPs) as a live attenuated malaria vaccine for humans may thus hold great promise, but a critical issue to be addressed is the proper complete attenuation of the vaccine (8, 26). Single-gene deletions may not be sufficient to completely attenuate the parasite, and therefore, vaccination could lead to breakthrough infections. For example, immunization of mice with *p52*-deficient sporozoites protected against subsequent infectious sporozoite challenge, but the immunizations led to sporozoite dose-dependent breakthrough infections in a substantial number of animals (10, 35).

In this study, we asked whether the deletion of P52 and P36 in the same parasite would lead to a complete block of infectivity for the mammalian host, thus not causing a breakthrough blood-stage infection. The tandem arrangement of the genes allowed the deletion of both genes (double knockout) with a single genetic manipulation. We used *P. yoelii* because its low 50% infective dose in BALB/c mice (<10 sporozoites) provides a more sensitive malaria infectivity model in mice compared to *P. berghei* infectivity in mice (2). The simultaneous deletion of P52 and P36 causes a complete loss of *P. yoelii* sporozoite infectivity for the rodent host even with a high-dose sporozoite inoculum. Double-knockout *p52*/*p36*-deficient sporozoites enter and traverse host cells normally but cannot establish a PV early in hepatocyte infection. Using this double knockout as a vaccine in mouse immunizations, we show its efficacy to induce sterile protection against infectious sporozoite challenge by intravenous injection or by mosquito bite.

MATERIALS AND METHODS

Experimental animals. Female Swiss Webster (SW) mice (6 to 8 weeks old) and female Wistar rats (5 weeks old) were purchased from Harlan Company (Indianapolis, IN). Female (6 to 8 weeks old) BALB/c mice were purchased from the Jackson Laboratory (Bar Harbor, ME). Animal handling was conducted according to institutional animal care and use committee-approved protocols.

Generation of Py52/Py36-deficient parasites. For the targeted deletion of the P52 and P36 genomic locus by replacement, two DNA fragments were amplified using *P. yoelii* 17XNL genomic DNA as a template: a 603-bp 5′ untranslated region fragment of *P. yoelii* P52 (Py52) and a 414-bp fragment in the 3′ end of the *P. yoelii* P36 (Py36) open reading frame (ORF). The primers used were Py52-5′RepF (5′-AATT*GGTACC*CAAATTAGTGCATGTATACAAGTAT-3′ [the KpnI site is in italics]) and Py52-5′RepR (5′-ATAT*CCTGCAGG*CAAACGGT AATAGTGGACATCAT-3′ [the SbfI site is in italics]) for the first fragment and Py36-3′RepF (5′-AATT*GGATCC*TGAAATAGATGCATATCCTGGG-3′ [the BamHI site is in italics]) and Py36-3′RepR (5′-AATT*ACTAGT*GTATGAATT GCGTGAGAAATGC-3′ [the SpeI site is in italics]) for the second fragment. Cloning into the plasmid b3D.DTĤ.D̂ targeting vector (provided by Andy Waters) resulted in plasmid Py52/36Repb3D.DTĤ.D̂. Transfection was performed by using a Nucleofector device (Amaxa GmbH). Approximately 1.0×10^7 purified *P. yoelii* mature schizonts were mixed with 14 μg of the replacement fragment excised by KpnI/SacII digestion per 10 μl of Tris-EDTA (pH 8.0) and 100 μl of Human T Cell Nucleofector solution (Amaxa GmbH). Parasites were transfected using the electroporation program U-033, which is available with the Nucleofector device, and injected intravenously into naïve SW recipient mice. Drug-resistant parasites were selected by pyrimethamine administered in the drinking water of mice (70 μg/ml). DNA genotyping by PCR of wild-type (wt) and *p52*/*p36*-deficient parasites was performed using primers specific for the wt locus (sense primer5′-GAATCAAATGAGCGCACACACAATG-3′ and antisense primer5′-GGTTTTCAATAATGTCATTCATGC-3′) and the *p52*/*p36*-deficient locus (sense primer5′-TGATGTTTTTTCCTTCAATTTCG-3′ and antisense primer5′-TTGTTCATACGCATATTTGTTATAG-3′). Two independent clones, *p52*/*p36*-deficient clone 1 (Cl1) and *p52*/*p36*-deficient Cl2, were obtained by limited dilution from independent transfection experiments. A wt clone that did not have the gene deletion but that underwent the same experimental manipulations was generated as a control parasite.

Reverse transcriptase PCR (RT-PCR). To evaluate transcript expression, 1.0×10^6 salivary gland wt clone sporozoites and *p52*/*p36*-deficient Cl1 and Cl2 sporozoites were collected. RNA was extracted using TRIzol reagent (Invitrogen) and treated with TURBO DNase (Ambion). cDNA synthesis was performed using the Super Script III Platinum 2-step qRT-PCR kit (Invitrogen). Py52, Py36, and *P. yoelii* CSP (PyCSP) gene-specific oligonucleotide primers were used in a standard PCR amplification (30 cycles). Sequences were as follows: sense primer5′-GAATCAAATGAGCGCACACACAATG-3′ and antisense primer5′-GGTTTTCAATAATGTCATTCATGC-3′ for P52, sense primer5′-TTACATACACACTTTACCTGGAG-3′ and antisense primer5′-GTAT GAATTGCGTGAGAAATGC-3′ for P36, and sense primer5′-AGCCCAAA GAAACTTAAACGAGC-3′ and antisense primer5′-GCCAAGTAATCTGTT GACTATATTTCGA-3′ for CSP.

Phenotypic analysis of Py52/Py36-deficient parasites in the mosquito. *Anopheles stephensi* mosquitoes were infected with Py52/Py36-deficient parasites and control wt clone parasites by blood feeding for 5 min on the first day and 15 min on the following day on infected SW mice and subsequently maintained under a cycle of 12.5 h light/11.5 h dark and 70% humidity at 24.5°C. Gametocyte exflagellation capacity was evaluated microscopically before mosquito blood meal. Infected mosquitoes were dissected (30 mosquitoes for each dissection) at days 10 and 14 (after the first infectious blood meal) to determine the mean number of midgut oocyst sporozoites and salivary gland sporozoites, respectively, per mosquito by using a hemocytometer.

In vitro analysis of infection. All the in vitro assays were conducted using the human hepatoma cell line HepG2 expressing the tetraspanin CD81 (HepG2-CD81) (28) cultured in Dulbecco's modified Eagle's medium with 10% fetal calf serum at 37°C and 5% CO_2. Infections were done by adding 5.0×10^4 sporozoites to 8.0×10^4 subconfluent HepG2-CD81 cells per well (Permanox eight-well chamber slide; Nalge Nunc International, Rochester, NY), except for the cell-wounding assay, where 3.0×10^4 sporozoites were used to infect 5.0×10^4 subconfluent HepG2-CD81 cells per well.

A double-staining test to differentiate sporozoites outside a host cell from sporozoites inside a host cell (hepatocyte entry) was performed as described

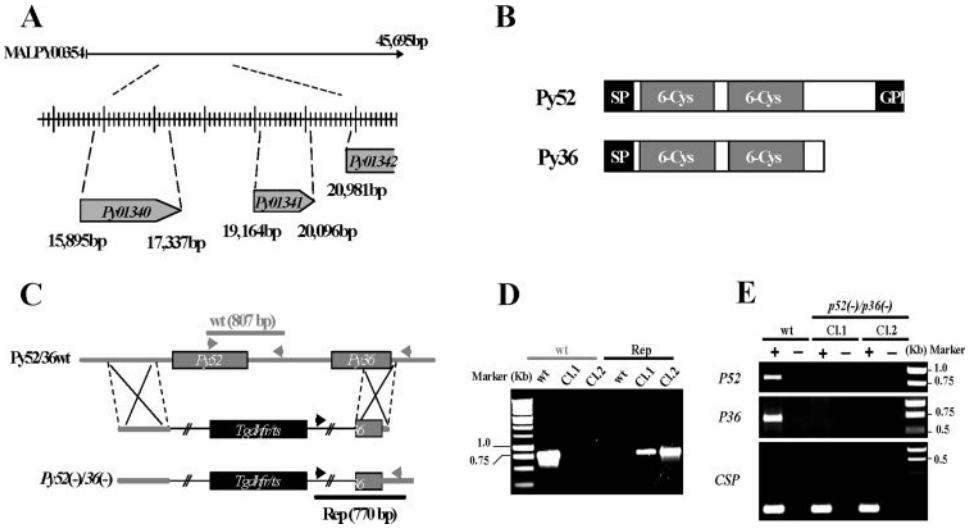

FIG. 1. Targeted gene disruption of P52 and P36 using a single-replacement strategy. (A) *P. yoelii* P52 (PY01340) and P36 (PY01341) are located in tandem on contig MALPY00354. (B) Predicted protein structure of P52 and P36. Each protein exhibits a signal peptide (SP) followed by two 6-Cys domains. In addition, P52 possesses a putative GPI anchor transfer peptide. (C) Schematic representation of the replacement strategy to generate the *p52*/*p36*-deficient parasites. The wild-type (wt) P52/P36 genomic locus was targeted with a replacement plasmid containing a 5′ untranslated region fragment of P52 and a 3′ fragment of the P36 ORF that flank the *Toxoplasma gondii* dihydrofolate reductase-thymidylate synthase-positive selectable marker. A recombination event (double crossover) resulted in the replacement of the P52 ORF and the 5′ part of the P36 ORF by the selection marker. wt and replacement-specific oligonucleotide primer combinations used for genotyping are indicated by arrows, and expected fragments are shown by gray and black lines. (D) PCR genotyping. Amplification with oligonucleotide primer combinations that can amplify only from the recombinant locus (Rep) confirmed the gene replacement. The wt-specific oligonucleotide primer combinations confirmed the absence of residual wt parasites in *p52*/*p36*-deficient Cl1 and Cl2. (E) The *p52*/*p36*-deficient parasites do not transcribe P52 and P36. The absence of P52 and P36 transcripts in *p52*/*p36*-deficient parasites was shown by RT-PCR using gene-specific oligonucleotide primers and salivary gland sporozoite RNA as a template. Gene-specific oligonucleotide primers for CSP were used as a positive control and amplified from wt and *p52*/*p36*-deficient sporozoite RNA. − indicates reactions without RT, and + indicates reactions with RT.

previously (27), with modifications. After 60 min of incubation, cells were fixed with 4% paraformaldehyde, blocked with phosphate-buffered saline (PBS)–1% fetal calf serum, and stained with anti-PyCSP 9D3 primary antibody (Ab), followed by Alexa Fluor 594 (red) goat anti-mouse immunoglobulin G (IgG) (Molecular Probes, Eugene, OR). After washing with PBS, cell membranes were permeabilized with 100% methanol at room temperature. Cells were again blocked and then stained with anti-PyCSP Ab followed by Alexa Fluor 488 (green) goat anti-mouse IgG secondary Ab. For the cell-wounding assay, *P. yoelii* wt, *p52*/*p36*-deficient sporozoites, and uninfected salivary gland extracts (mock) were added to subconfluent HepG2-CD81 cell cultures with 2 mg/ml of fluorescein isothiocyanate (FITC)-dextran (Invitrogen-Molecular Probes, Eugene, OR) in each culture. After a 3-min centrifugation at 500 × *g*, cultures were incubated for 1 h and washed three times with PBS to remove extracellular dextran. They were then further incubated for 3 h in normal medium. For qualitative microscopic evaluation, cell cultures were fixed with 4% paraformaldehyde and mounted. For flow cytometric analyses, cultures were washed twice and incubated with trypsin for 5 min at 37°C. Each trypsinized culture was mixed with 200 μl of complete medium and pelleted. Cell pellets were resuspended in 100 μl of complete medium and subjected to flow cytometry (Cytopia, Seattle, WA). Analysis of data was performed using the flow cytometry analysis program FlowJo version 7.0.3 (TreeStar, Inc., Ashland, OR).

For the infection assay, sporozoites were incubated for 2 h with HepG2-CD81 cells. The cultures were fixed with 4% paraformaldehyde, followed by permeabilization with 100% methanol for 10 min at room temperature. Double staining was performed using anti-PyCSP 9D3 primary Ab, followed by Alexa Fluor 488 and anti-*P. yoelii* UIS4 (PyUIS4) primary Ab and Alexa Fluor 594 goat anti-rabbit IgG (Molecular Probes, Eugene, OR).

For the LS development assay, infections were maintained for 43 h, and the medium was replaced both 3 h and 20 h postinfection (p.i.). Fixation and permeabilization conditions were identical to those of the infection assay described above. The double staining was performed using anti-PyUIS4 primary Ab following by Alexa Fluor 594 and anti-*P. yoelii* heat shock protein 70 (PyHsp70) Ab directly conjugated with Alexa Fluor 488. For each experiment, cells were stained with 4′,6′-diamidino-2-phenylindole (DAPI) to visualize the DNA and mounted with antifade reagent (FluoroGuard; Bio-Rad, Hercules, CA). Preparations were analyzed using a fluorescence inverted microscope (Eclipse TE2000-E; Nikon), and images were acquired using Olympus 1X70 Delta Vision deconvolution microscopy.

For thin-section transmission electron microscopy, 10^6 wt and *p52*/*p36*-deficient sporozoites were used to infect 10^6 subconfluent HepG2-CD81 cells. One hour p.i., cells were fixed with 2.5% glutaraldehyde (Electron Microscopy Sciences, Hatfield, PA) in 0.1 M sodium cacodylate buffer (pH 7.4) for 1 h at room temperature and processed as described previously (25) before examination with a Philips (Eindhoven, The Netherlands) 410 electron microscope under 80 kV.

In vivo analysis of infection. To analyze in vivo sporozoite infection and LS development, mice were injected by intravenous (i.v.) injection with 2.0×10^6 wt or *p52*/*p36*-deficient sporozoites. For each parasite population, livers were harvested at time points 2 and 6 h postinjection. Livers were washed extensively with PBS and fixed in 4% paraformaldehyde. Several 50-μm sections were made from each liver using a Vibratome apparatus (Ted Pella Inc., Redding, CA). Preparations were stained with anti-PyUIS4 primary Ab followed by Alexa Fluor 594 and with anti-PyCSP 9D3 primary Ab followed by Alexa Fluor 488. Preparations were analyzed using a fluorescence inverted microscope (Eclipse TE2000-E; Nikon), and images were acquired using Olympus 1X70 Delta Vision deconvolution microscopy.

In vivo infectivity of Py52/Py36-deficient sporozoites. To determine the in vivo infectivity of Py52/Py36-deficient sporozoites, BALB/c mice were infected either by mosquito bite (1 mouse/15 mosquitoes/10-min feeding) or by i.v. injection of sporozoites (1.0×10^4, 5.0×10^4, or 1.0×10^5 sporozoites) resuspended in 100 μl of RPMI 1640. Wistar rats were infected by i.v. injection of 1.0×10^5 sporozoites resuspended in 100 μl of RPMI 1640. Parasitemia was evaluated by Giemsa-stained thin blood smears starting at the second day after sporozoite inoculation. Animals were evaluated up to 20 days after sporozoite injection.

Immunization and challenge experiments. Naïve BALB/c mice were immunized and boosted by i.v. injection of Py52/Py36-deficient Cl2 sporozoites. The immunized mice were challenged by infected mosquito bite (1 mouse/15 mosquitoes/10-min feeding) or with 1.0×10^4 wt sporozoites by i.v. injection. Animals were monitored for blood-stage parasitemia by daily blood smears.

TABLE 1. Phenotypic analysis of Py52/Py36-deficient sporozoites and LSs

Parasite population	No. of salivary gland sporozoites per mosquito[a]	Hepatocyte entry (no. of cells)[b]		No. of LSs at 43 h[c]
		Outside	Inside	
P. yoelii wt clone	30,389 ± 13,241	593 ± 58.63	502 ± 61.82	278.25 ± 79.88
Py52/Py36-deficient Cl1	24,031 ± 11,834	849.66 ± 136.64	272 ± 54.5	1 ± 1
Py52/Py36-deficient Cl2	21,822 ± 7,639	842.33 ± 75.79	284 ± 79	1 ± 1.41
P. yoelii wt clone + CytD[d]	NA	1,046.66 ± 47.89	27 ± 9.53	ND

[a] The mean number of sporozoites was determined from at least three independent mosquito feeding experiments at day 14 after the infectious blood meal. NA, not applicable.
[b] For this specific test, hepatocyte entry is defined as the sporozoite's ability to cross a host cell membrane and to enter the cell. Sporozoites were counted in at least three different wells. Eight fields per well were examined.
[c] Experiments were done in duplicate. ND, not determined.
[d] As a negative control, wt sporozoite motility was inhibited by treatment with 1 μM cytochalasin D (CytD) for 15 min at 37°C.

RESULTS

Genomic organization and gene-targeting strategy. The Py52 (GenBank accession no. AF390552 and PlasmoDB accession no. PY01340) and Py36 (GenBank accession no. AABL01000353 and PlasmoDB accession no. PY01341) genes are paralogous tandemly arranged genes on contig MALPY00354 (Fig. 1A). They are separated by 1,827 bp and have ORFs of 1,440 bp and 930 bp, respectively. The Py52 gene encodes a predicted 52-kDa protein, and the Py36 gene encodes a predicted 35.3-kDa protein. P52 and P36 have a predicted N-terminal cleavable signal peptide followed by two 6-Cys domains, but unlike P36, P52 exhibits a C-terminal hydrophobic sequence predicted to be a putative GPI anchor attachment signal (Fig. 1B).

A replacement-targeting plasmid (Fig. 1C) was made to simultaneously delete the endogenous P52 and P36 genes by double-crossover homologous recombination (17). Two independent transfection experiments were performed using the Nucleofector device. Transfected parasites were intravenously injected into naïve SW mice. At day 9 after inoculation, the first pyrimethamine-resistant blood-stage parasites were detected in both mice. After identification of the replacement event by PCR (data not shown), the parental parasite populations were used to clone *p52*/*p36*-deficient parasites. PCR analysis of genomic DNA from *p52*/*p36*-deficient parasite clones detected no residual wt genotype (Fig. 1D). Two independent *p52*/*p36*-disrupted clones, *p52*/*p36*-deficient Cl1 and Cl2, were generated and used for phenotypic analyses.

***p52*/*p36*-deficient sporozoites develop normally in the mosquito vector.** The successful selection of *p52*/*p36*-deficient par-

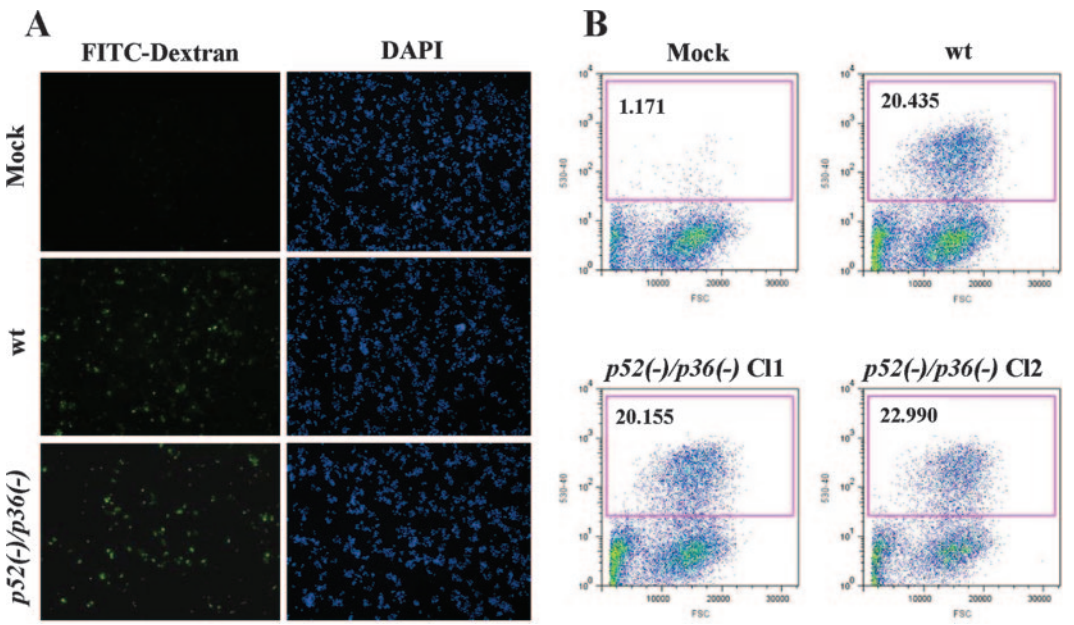

FIG. 2. *p52*/*p36*-deficient sporozoites traverse and wound cells normally. (A) Overview of infected HepG2-CD81 cultures showing FITC-positive (green) wounded cells as a result of wt or *p52*/*p36*-deficient sporozoite traversal. DAPI (blue) visualizes the nuclei. (B) Quantification of cell-wounding activity using flow cytometry reveals a similar level of traversal activity in wt and *p52*/*p36*-deficient sporozoites. The assay was repeated six times for each sample. Approximately 3.0×10^4 sporozoites were incubated with 5.0×10^4 subconfluent HepG2-CD81 cells per well in the presence of FITC-dextran. The *x* axis represents the forward-scatter properties of the cells, while the *y* axis represents the green fluorescence. The numbers of wounded cells (percent) are shown in the upper left corners of the graphs. Approximately 20% of the HepG2-CD81 cells inoculated with wt and *p52*/*p36*-deficient (Cl1 and Cl2) sporozoites were fluorescent, i.e., wounded. Mock infections were done by incubating HepG2-CD81 cells with uninfected mosquito salivary gland preparations.

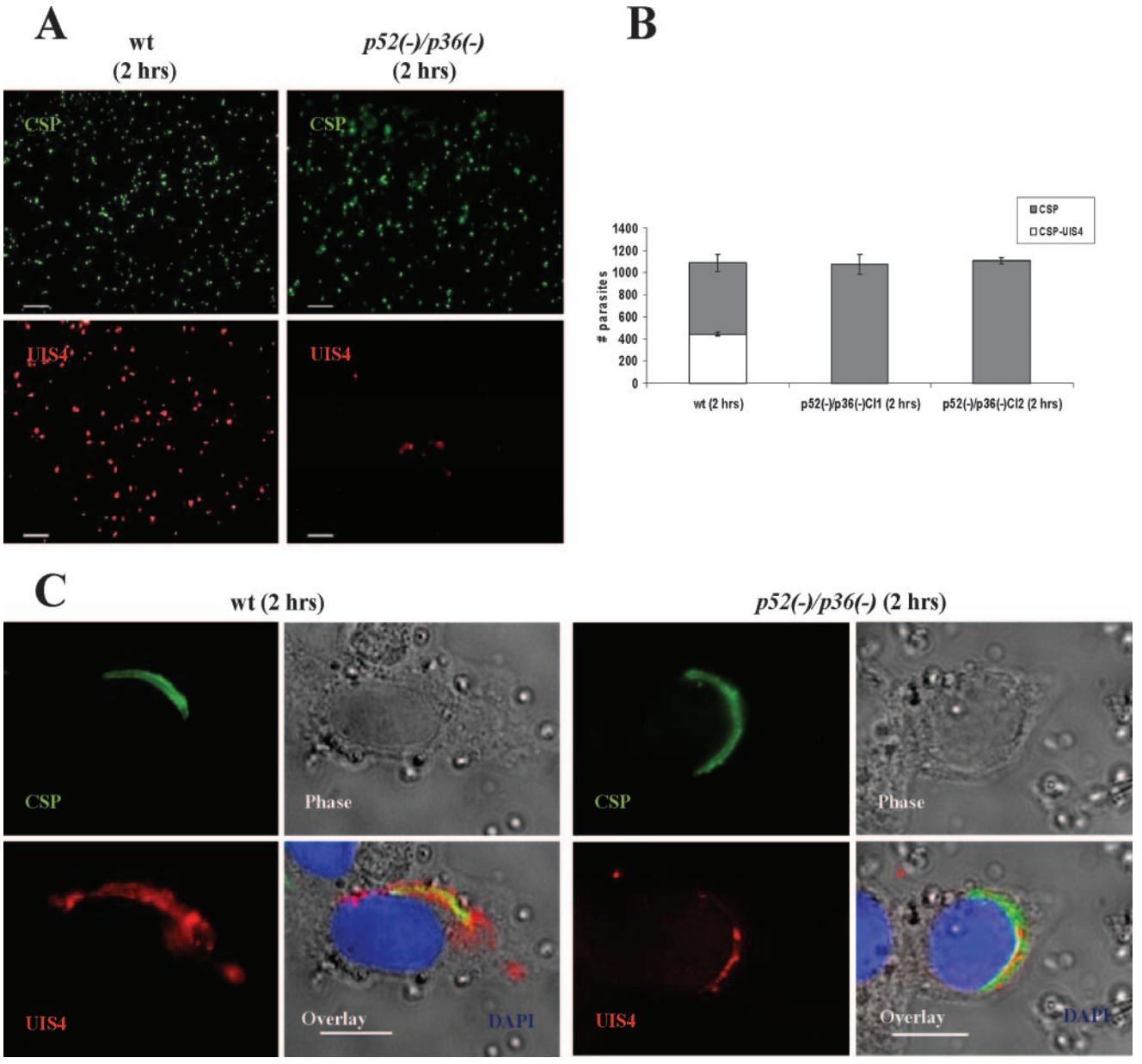

FIG. 3. *p52/p36*-deficient parasites fail to infect hepatocytes with the formation of a PV in vitro. Immunofluorescence assay with infected HepG2-CD81 cells using Abs to UIS4, a PVM-resident protein, allows the detection of the parasite PVM 2 h p.i. (A) Low-magnification images showing wt parasite staining with anti-UIS4 and anti-CSP Abs (left panels). UIS4 expression is not apparent in *p52/p36*-deficient parasites at the low magnification shown in the right panels (scale bar, 40 μm). (B) Microscopic quantification reveals that ~40% of wt parasites show strong UIS4 staining of the PVM and show CSP staining of the parasite surface. The remaining ~60% of wt parasites stained with CSP represent extracellular sporozoites and sporozoites in cell traversal mode. *p52/p36*-deficient parasites were detected by anti-CSP staining only. Numbers shown are means ± standard deviations of counting 1.0×10^3 parasites per well in three wells. (C) Higher magnification shows typical peripheral localization of UIS4 in the PVM surrounding an intracellular wt parasite. Intracellular *p52/p36*-deficient parasites occasionally exhibit a signal of UIS4 staining within the sporozoite (scale bar, 10 μm). Cells were labeled with DAPI (blue) to visualize the nuclei.

asites indicated that P52 and P36 are not involved in blood-stage replication. Also, the abilities of gametocytes to exflagellate in vitro were similar in wt and *p52/p36*-deficient parasites (data not shown). We next analyzed sporozoite development and salivary gland invasion of wt and *p52/p36*-deficient parasites in the mosquito. No significant difference was detected between the mean numbers of wt and *p52/p36*-deficient Cl1 and Cl2 sporozoites in midguts (data not shown) and in salivary glands (Table 1). RT-PCR confirmed the lack of P52 and P36 gene transcripts in *p52/p36*-deficient salivary gland sporozoites (Fig. 1E). RT-PCR using CSP gene oligonucleotide primers was used as a positive transcript control, and CSP expression appeared to be unchanged in *p52/p36*-deficient salivary gland sporozoites (Fig. 1E).

***p52/p36*-deficient sporozoites traverse cells normally but fail to establish an infection in vitro.** We investigated the ability of

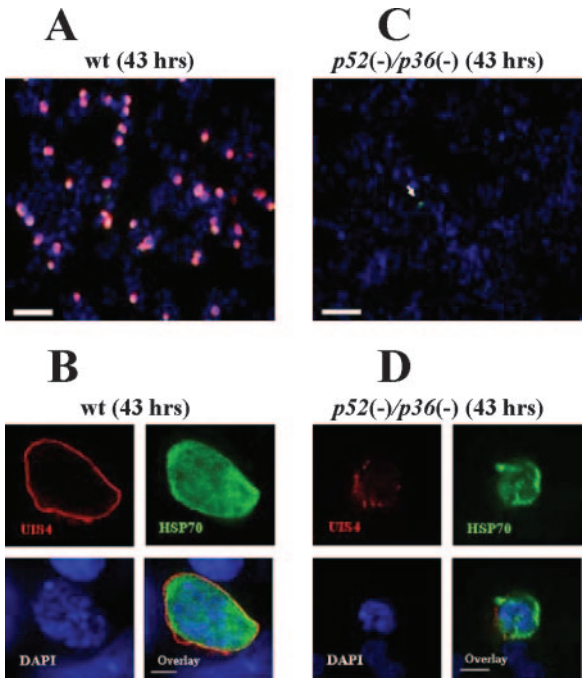

FIG. 4. *p52/p36*-deficient parasites show a severe defect in LS development in vitro. *P. yoelii* wt LSs grow in HepG2-CD81 cells and complete development, but *p52/p36*-deficient LSs do not grow and do not persist in infected cells. (A) Forty-three hours p.i., wt LSs have developed to the late schizont stage. LSs are visualized by staining with anti-UIS4 Abs (red) and anti-Hsp70 Abs (green). Nuclei were visualized with DAPI (scale bar, 30 μm). (B) Higher magnification shows a late wt LS with multiple nuclei entirely surrounded by a PVM that is revealed by anti-UIS4 staining (scale bar, 5 μm). (C) *p52/p36*-deficient parasites do not grow in HepG2-CD81 cells. A small *p52/p36*-deficient growth-arrested LS is indicated by the white arrow (scale bar, 30 μm). (D) Higher magnification of a growth-arrested *p52/p36*-deficient parasite 43 h p.i. does not show a typical PVM using UIS4 staining. Some UIS4-positive vesicular structures are visible (scale bar, 5 μm).

Py52/Py36-deficient sporozoites to enter host cells in vitro using HepG2-CD81 cells. Our choice to use the HepG2 hepatoma cells expressing a human CD81 is based on their high susceptibility to *P. yoelii* sporozoite infection and efficient LS development (28). The level of hepatocyte entry was determined by counting the number of sporozoites inside host cells relative to those outside host cells (Table 1). On average, 1,000 sporozoites were counted within a well an hour after infection. The number of intracellular *p52/p36*-deficient parasites showed a ~50% reduction compared to wt sporozoites (Table 1). We next examined the cell traversal ability of *p52/p36*-deficient sporozoites. This activity was evaluated by the quantification of wounded HepG2-CD81 cells that had taken up FITC-conjugated dextran (20) (Fig. 2A) by using flow cytometry. Several independent experiments with wt and *p52/p36*-deficient sporozoites consistently showed that ~20% of the total number of cells per culture were fluorescent, i.e., had been wounded (Fig. 2B). These data demonstrate the ability of *p52/p36*-deficient sporozoites to traverse cells normally. The successful infection of hepatocytes that leads to productive LS development requires the formation of a PV compartment during invasion by sporozoites. To assess this activity, we performed immunofluorescence analysis to localize UIS4, a resident protein of the PVM and in its associated tubovesicular network (21). Two hours after infection of HepG2-CD81 cells with wt sporozoites, early LSs exhibiting circumferential UIS4 staining were easily detectable (Fig. 3A). Strikingly, *p52/p36*-deficient parasites did not show this UIS4 staining pattern (Fig. 3A). Quantitative analysis showed a complete absence of circumferential UIS4 staining in *p52/p36*-deficient parasites (Fig. 3B). In wt parasites, we found that ~40% of the parasites had infected host cells and exhibited circumferential UIS4 staining. Further analysis using deconvolution microscopic observations at higher magnifications showed a strong UIS4 staining pattern entirely surrounding the invaded wt sporozoites (Fig. 3C). However, intracellular *p52/p36*-deficient sporozoites exhibited weak internal staining for UIS4 (Fig. 3C). Next, we investigated whether *p52/p36*-deficient parasites were able to develop

TABLE 2. Py52/Py36-deficient sporozoites cannot infect the mammalian host

P. yoelii parasite population	No. of injected sporozoites[a]	No. of infected mice/ no. of injected mice/ prepatency[b]	*P* value[c]
Mouse infection			
wt clone	1.0×10^4	24/24/3	
p52/p36-deficient Cl1	1.0×10^4	0/5/—	<0.0001
p52/p36-deficient Cl2	1.0×10^4	0/58/—	<0.0001
wt clone	1.0×10^5	6/6/2.5	
p52/p36-deficient Cl1	1.0×10^5	0/3/—	<0.1
p52/p36-deficient Cl2	1.0×10^5	0/5/—	<0.01
p52/p36-deficient Cl2	5.0×10^4	0/10/—	ND
wt clone	Mosquito bite	3/3/d3	
p52/p36-deficient Cl1	Mosquito bite	0/5/—	<0.1
p52/p36-deficient Cl2	Mosquito bite	0/5/—	<0.1
Rat infection			
wt clone	1.0×10^5	5/5/2.5	
p52/p36-deficient Cl2	1.0×10^5	0/5/—	<0.01

[a] Sporozoites were injected intravenously in the tail of mice or by mosquito bite.
[b] Prepatency indicates the number of days after sporozoite injection until detection of a single erythrocytic stage by microscopic blood smear examination.
[c] *P* values were determined by Fisher's exact test. ND, not determined.

as LS inside host cells by the incubation of infected HepG2-CD81 cells for 43 h. As expected, the wt parasite-infected cells showed a high number of late LS schizonts (Fig. 4A) fully surrounded by UIS4 (Fig. 4B). However, no *p52/p36*-deficient late-LS schizonts were detected after 43 h. We sporadically observed small growth-arrested parasites that did not show typical UIS4 staining (Fig. 4C and D).

***p52/p36*-deficient sporozoites fail to infect the mammalian host.** In order to analyze the relevance of the observed defect in *p52/p36*-deficient sporozoite host cell infection in vivo, we investigated the ability of the *p52/p36*-deficient sporozoites to infect the mammalian host. BALB/c mice were intravenously inoculated with different doses (1.0×10^4, 5.0×10^4, or 1.0×10^5) of *p52/p36*-deficient sporozoites. Mice did not develop a blood-stage infection even when inoculated with an extremely high dose of 1.0×10^5 sporozoites (Table 2). This was further confirmed by infecting mice with mosquito bites (Table 2). In addition, rats inoculated with a single dose of 1.0×10^5 *p52/p36*-deficient sporozoites also did not develop a blood-stage infection. To evaluate the cellular phenotype of *p52/p36*-deficient parasites in vivo, microscopic analysis and quantification of infected liver sections in comparison to wt infections were performed. Intrahepatocytic wt parasites were identified by CSP and UIS4 immunostaining (Fig. 5A). We could also detect *p52/p36*-deficient parasites in liver sections by CSP staining, but they did not show UIS4 staining. Approximately 75% of the total wt parasites but no *p52/p36*-deficient parasites detected at 2 h p.i. showed UIS4-postive circumferential staining, (Fig. 5A and B). Furthermore, at 2 h p.i., we detected fewer *p52/p36*-deficient parasites (Fig. 5B). We did not detect any *p52/p36*-deficient parasites in the host liver at 6 h p.i. (data not shown).

***p52/p36*-deficient parasites cannot establish a parasitophorous vacuole.** The absence or abnormal localization of the PVM protein UIS4 in intracellular *p52/p36*-deficient parasites indicated a possible lack of the PVM. To further address this issue, we performed an electron microscopic analysis of intracellular wt and *p52/p36*-deficient parasites 1 h after infection of HepG2-CD81 cells. Intracellular wt parasites were clearly surrounded by a PVM (Fig. 6A). Out of 22 parasites evaluated by electron microscopy, 20 exhibited a PVM, and 2 appeared free in the cytoplasm. The latter may represent sporozoites in the process of cell traversal. However, all of the 14 intracellular *p52/p36*-deficient parasites observed lacked a PVM and were in direct contact with the host cell cytoplasm or freely exposed to the nucleoplasm (Fig. 6B and C). Together, the data demonstrate that *p52/p36*-deficient parasites do not possess a PVM early in infection.

Immunization with *p52/p36*-deficient sporozoites induces sterile protection against wt sporozoite challenge. The fact that the *p52/p36*-deficient parasites show a complete defect in productive liver infection prompted us to test their potential as a preerythrocytic GAP malaria vaccine. Different immunization/challenge experiments were performed (Table 3). Each set of experiments was carried out with age-matched mice including naïve mice used as a control to verify the infectivity of the sporozoite challenge dose. Mice immunized with three doses of 1.0×10^4 *p52/p36*-deficient sporozoites showed complete protection against challenge with 1.0×10^4 wt sporozoites 7 and 30 days after the last immunization. Furthermore, the same triple-immunization regimen conferred complete protection against sporozoite

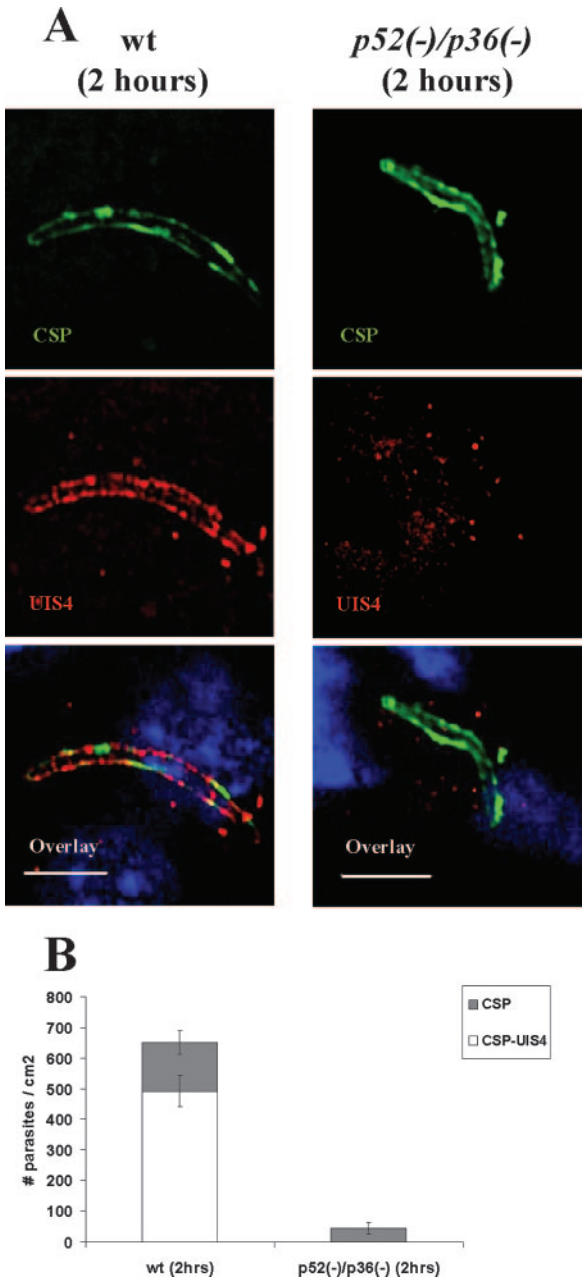

FIG. 5. *p52/p36*-deficient parasites fail to establish infection in the host liver. (A) Indirect immunofluorescence assay of wt and *p52/p36*-deficient parasites detected in the host liver at 2 h p.i. The upper panels show intracellular wt parasite or *p52/p36*-deficient parasite staining with anti-CSP Abs. The PVM is visualized in wt parasites using anti-UIS4 Ab staining, but UIS4 staining is not discernable in *p52/p36*-deficient parasites, indicating a PVM deficiency (middle panels). The overlay of UIS4 staining, CSP staining, and nuclear DAPI staining is shown in the bottom panels (scale bar, 20 μm). (B) Quantification of liver infections. Numbers shown are means ± standard deviations of wt parasites and *p52/p36*-deficient parasites detected in three discontinuous sections of livers of BALB/c mice 2 h p.i. *p52/p36*-deficient parasites were detected at greatly reduced numbers (~90% reduction) compared to wt parasites and did not show UIS4 staining ($P < 0.0001$, Fisher's exact test). Approximately 75% of wt parasites detected at 2 h p.i. showed UIS4-positive staining and CSP-positive staining.

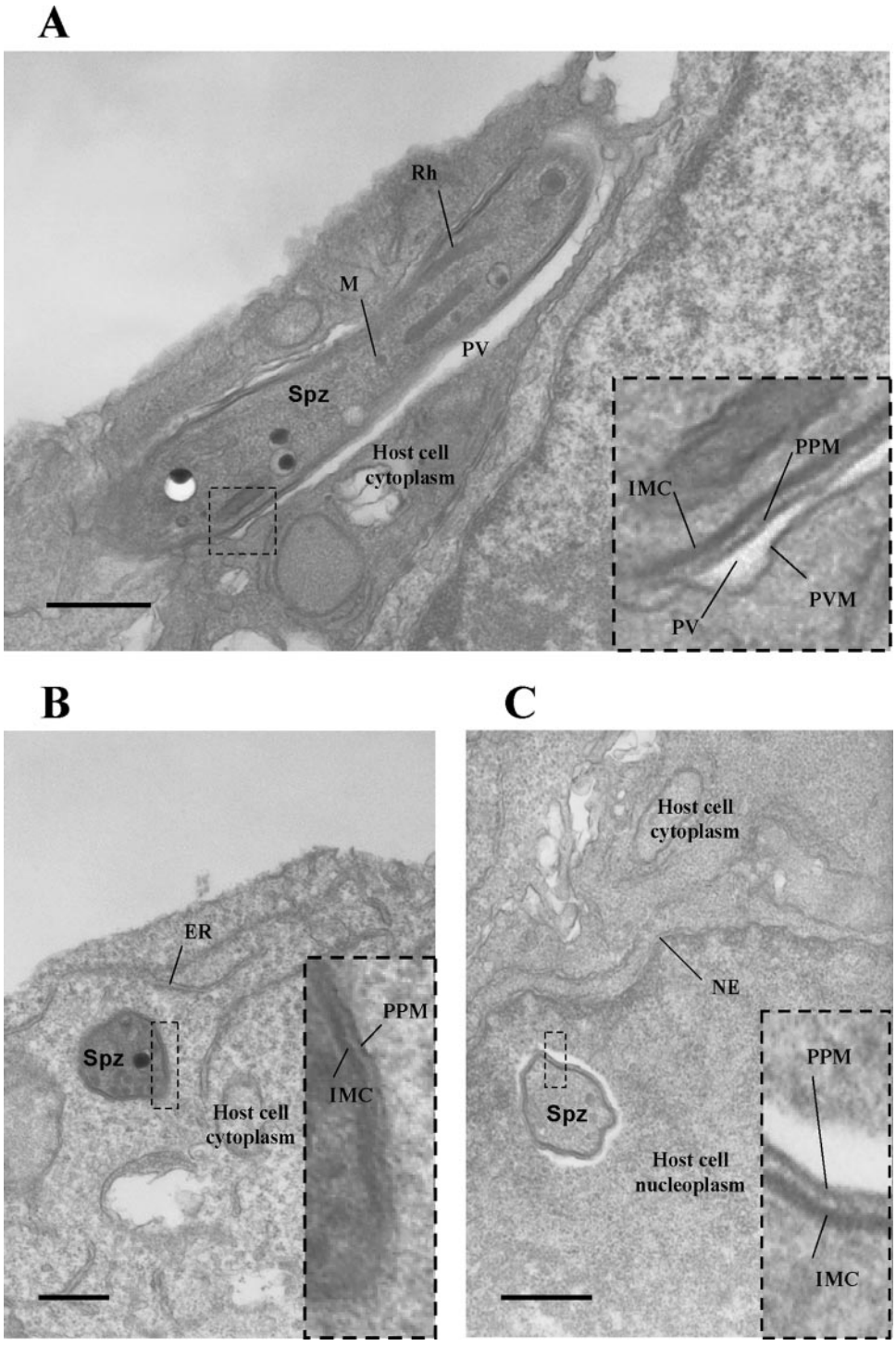

FIG. 6. Electron microscopic analysis confirms that *p52*/*p36*-deficient parasites cannot form a parasitophorous vacuole. (A) wt sporozoite (longitudinal view) within a HepG2-CD81 cell 1 h after infection. The parasite is surrounded by a PVM. (B) *p52*/*p36*-deficient sporozoite (transversal view) within a HepG2-CD81 cell 1 h after infection. The parasite lacks a PVM and appears to be in direct contact with the host cell cytoplasm. (C) A *p52*/*p36*-deficient sporozoite (transversal view) was also detected within the host cell nucleus, surrounded by nucleoplasm. All scale bars are 0.5 μm. The inset boxes show higher magnifications of the boxed areas within the overview images. ER, endoplasmic reticulum; IMC, inner membrane complex; M, microneme; NE, nuclear envelope; PPM, parasite plasma membrane; Spz, sporozoite; Rh, rhoptry.

TABLE 3. Protection of BALB/c mice immunized with Py52/Py36-deficient sporozoites against challenge with wt *P. yoelii* sporozoites

Expt	No. of primary *p52*/*p36*-deficient sporozoites	No. of *p52*/*p36*-deficient sporozoites injected for first boost (day)/no. injected for second boost (day)[a]	Challenge dose of wt sporozoites (day)[b]	No. of protected mice/no. of challenged mice/prepatency[c]	*P* value[d]
1	1.0×10^4	1.0×10^4 (7)/1.0×10^4 (14)	1.0×10^4 (7)	8/8/—	<0.01
1 (control)			1.0×10^4	0/4/3	
2	1.0×10^4	1.0×10^4 (7)/1.0×10^4 (14)	Mosquito bite (7)	5/5/—	<0.1
2 (control)			Mosquito bite	0/3/3	
3	1.0×10^4	1.0×10^4 (7)/1.0×10^4 (14)	1.0×10^4 (30)	7/7/—	<0.01
3 (control)			1.0×10^4	0/4/3	

[a] Days after primary injection are shown in parentheses.
[b] Immunized mice were challenged with wt *P. yoelii* sporozoites by i.v. injection or mosquito bite. For each experiment, sporozoites were from the same mosquito batch. Days after final boost are shown in parentheses.
[c] Prepatency is the number of days after sporozoite inoculation until detection of a single erythrocytic stage by blood smear examination.
[d] *P* values were determined by Fisher's exact test.

challenge by mosquito bite. These results indicate that *p52*/*p36*-deficient sporozoites are able to induce sterile protection against a challenge with high doses of infectious sporozoites as well as against natural mosquito infection.

DISCUSSION

Only a small number of human malaria parasite salivary gland sporozoites (23, 33) are needed to infect the host. Therefore, sporozoite infection is highly efficient despite the complexity of its journey to the liver. The *P. yoelii* BALB/c mouse malaria model is a good infectivity model because of its low 50% infective dose of less than 10 sporozoites (2). By simultaneous deletion of two putative sporozoite 6-Cys superfamily ligands, P52 and P36, we created mutant *P. yoelii* parasites that cannot successfully infect the mammalian host. We showed that the *p52*/*p36*-deficient sporozoites are unable to cause a blood-stage infection even when inoculated at high doses. Previous studies using *P. berghei* showed that single-knockout *p52*- or *p36*-deficient sporozoites remained partially infective and caused blood-stage infection (10). Approximately 5% of rats inoculated with 3.0×10^3 *p52*-deficient sporozoites and ~40% of rats inoculated with 3.0×10^3 *p36*-deficient sporozoites became blood-stage parasitemic. The rate of blood-stage infection increased with the inoculation of higher sporozoite doses and reached 60% in the case of 1.0×10^5 *p52*-deficient sporozoites and 100% in the case of 3.0×10^4 *p36*-deficient sporozoites (10). The partial infectivity of *P. berghei* P52 (*p52*)-deficient sporozoites was also shown by using C57BL/6 mice, with 10% of mice becoming parasitemic (35). Although the *p52*-deficient sporozoites conferred protection against infectious sporozoite challenge (35), they were not sufficiently attenuated to consider them as a candidate GAP vaccine because of the relatively high incidence of breakthrough infections. We have shown herein that the simultaneous deletion of P52 and P36 creates completely attenuated parasites. Despite the fact that previous studies and our study used distinct *Plasmodium* rodent models, the significant differences between the single- and double-knockout sporozoite infectivity profiles may allow us to think that P52 and P36 have partially redundant functions. However, P36 is a predicted secreted protein, while P52 is a predicted GPI-anchored protein, thus making it difficult to envision how each protein could partially compensate for the loss of the other. A similar case where individual disruptions of paralogous genes showed a comparable but not complete phenotypic defect was described for *P. berghei* ookinete surface proteins P25 and P28 (32). These proteins are partially redundant, with similar functions during the ookinete/oocyst transition. The simultaneous disruption of these genes showed an almost complete loss (>99%) of oocysts.

A phenotypic analysis of *p52*- and *p36*-deficient sporozoites reported previously by Ishino et al. (10) showed that the single-knockout *P. berghei* parasites could infect HepG2 cells with the formation of a PVM albeit with reduced efficiency. That group also observed a significant increase in the cell traversal activity of single-knockout parasites. Those authors speculated that disrupted parasites fail to switch to the "infection mode" and keep traversing host cells. Our observations with *P. yoelii p52*/*p36*-deficient sporozoites did not show an increase in traversal activity upon rigorous quantification by flow cytometry. Importantly, by studying the PVM early in infection, we demonstrate that *p52*/*p36*-deficient parasites fail to form a PVM. Thus, it is likely that P52 and P36 are critical in a pathway that leads to the formation of the PVM. We have used HepG2 cells expressing human CD81, which support efficient infection and complete development by *P. yoelii*. This is not the case for HepG2 cells that lack CD81. wt *P. yoelii* sporozoites traverse HepG2 cells normally but fail to form a PV (28). Here, we have shown that *p52*/*p36*-deficient sporozoites traverse HepG2-CD81 cells but fail to form a PV. Therefore, it is tempting to speculate on potential ligand-receptor interactions between P52/P36 proteins and CD81, which may be needed for PV induction. However, this needs to be addressed experimentally. *p52*/*p36*-deficient parasites remain free in the host cell cytoplasm or move on to penetrate the host cell nucleus. It is possible that the absence of the PVM as a controlled and highly organized LS-hepatocyte interface prevents the parasites' ability to establish an efficient system of nutrient uptake and that this leads to growth arrest. In addition, PVM-free LS could be prone to attack by the host cell and may therefore quickly be eliminated. In agreement with this scenario, we did not observe any growth-arrested parasites in vivo 6 h p.i. Whether the host hepatocyte containing the *p52*/*p36*-deficient parasites undergoes apoptosis, as has been observed previously by van Dijk et al. for *p52*-deficient-parasite-infected hepatocytes (35), or whether the host cell remains viable and eliminates the PVM-free parasite requires further investigation.

Parasites carrying deletions of the LS PVM proteins UIS3 or UIS4 showed severe defects in LS growth (21, 22) and thus appear superficially similar to *p52/p36*-deficient parasites. However, we have recently shown that *uis3*- and *uis4*-deficient parasites do form a PVM upon hepatocyte entry (30). Thus, the growth deficiencies of *uis3*- and *uis4*-deficient parasites are caused by the absence of the respective proteins in the PVM but not the absence of the PVM itself, as shown here for *p52/p36*-deficient parasites.

Immunizations with *uis3*- and *uis4*-deficient sporozoites completely protected against subsequent infectious sporozoite challenge (21, 22, 30). In the present study, a triple-immunization regimen with *p52/p36*-deficient sporozoites completely protected against intravenous sporozoite injection and mosquito bite challenge. Thus, GAPs with distinct biological characteristics could be used as protective vaccines. It will be of interest to compare the vaccine potencies of the now available GAPs and the relationship of protection and their biological characteristics. This will improve our understanding of the immune mechanisms that mediate sterile protection against malaria infection and will provide critical information on the path forward to a safe *Plasmodium falciparum* GAP vaccine that effectively protects humans.

ACKNOWLEDGMENTS

We thank J. Whisler, M. Roberts, and C. Kungkagam for expert technical assistance with mosquito rearing and N. Lejarcegui for expert technical assistance with flow cytometry and data analysis. We thank Dominique Mazier for providing us with the HepG2-CD81 cell line.

This work is partially supported by the Bill and Melinda Gates Foundation through the Foundation at the National Institutes of Health Grand Challenges in Global Health Initiative. S.H.I.K. is an inventor listed on U.S. patent 7,22,179 and international patent application PCT/US2004/043023, each titled "Live Genetically Attenuated Malaria Vaccine."

REFERENCES

1. **Baer, K., M. Roosevelt, A. B. Clarkson, Jr., N. van Rooijen, T. Schnieder, and U. Frevert.** 2007. Kupffer cells are obligatory for *Plasmodium yoelii* sporozoite infection of the liver. Cell. Microbiol. **9:**397–412.
2. **Belmonte, M., T. R. Jones, M. Lu, R. Arcilla, T. Smalls, A. Belmonte, J. Rosenbloom, D. J. Carucci, and M. Sedegah.** 2003. The infectivity of *Plasmodium yoelii* in different strains of mice. J. Parasitol. **89:**602–603.
3. **Carter, R., A. Coulson, S. Bhatti, B. J. Taylor, and J. F. Elliott.** 1995. Predicted disulfide-bonded structures for three uniquely related proteins of *Plasmodium falciparum*, Pfs230, Pfs48/45 and Pf12. Mol. Biochem. Parasitol. **71:**203–210.
4. **Eksi, S., B. Czesny, G. J. van Gemert, R. W. Sauerwein, W. Eling, and K. C. Williamson.** 2006. Malaria transmission-blocking antigen, Pfs230, mediates human red blood cell binding to exflagellating male parasites and oocyst production. Mol. Microbiol. **61:**991–998.
5. **Frevert, U., S. Engelmann, S. Zougbede, J. Stange, B. Ng, K. Matuschewski, L. Liebes, and H. Yee.** 2005. Intravital observation of *Plasmodium berghei* sporozoite infection of the liver. PLoS Biol. **3:**e192.
6. **Frevert, U., I. Usynin, K. Baer, and C. Klotz.** 2006. Nomadic or sessile: can Kupffer cells function as portals for malaria sporozoites to the liver? Cell. Microbiol. **8:**1537–1546.
7. **Gerloff, D. L., A. Creasey, S. Maslau, and R. Carter.** 2005. Structural models for the protein family characterized by gamete surface protein Pfs230 of Plasmodium falciparum. Proc. Natl. Acad. Sci. USA **102:**13598–13603.
8. **Good, M. F.** 2005. Genetically modified *Plasmodium* highlights the potential of whole parasite vaccine strategies. Trends Immunol. **26:**295–297.
9. **Ishino, T., Y. Chinzei, and M. Yuda.** 2005. A *Plasmodium* sporozoite protein with a membrane attack complex domain is required for breaching the liver sinusoidal cell layer prior to hepatocyte infection. Cell. Microbiol. **7:**199–208.
10. **Ishino, T., Y. Chinzei, and M. Yuda.** 2005. Two proteins with 6-Cys motifs are required for malarial parasites to commit to infection of the hepatocyte. Mol. Microbiol. **58:**1264–1275.
11. **Ishino, T., K. Yano, Y. Chinzei, and M. Yuda.** 2004. Cell-passage activity is required for the malarial parasite to cross the liver sinusoidal cell layer. PLoS Biol. **2:**E4.
12. **Kaiser, K., N. Camargo, I. Coppens, J. M. Morrisey, A. B. Vaidya, and S. H. Kappe.** 2004. A member of a conserved *Plasmodium* protein family with membrane-attack complex/perforin (MACPF)-like domains localizes to the micronemes of sporozoites. Mol. Biochem. Parasitol. **133:**15–26.
13. **Kaiser, K., K. Matuschewski, N. Camargo, J. Ross, and S. H. Kappe.** 2004. Differential transcriptome profiling identifies *Plasmodium* genes encoding pre-erythrocytic stage-specific proteins. Mol. Microbiol. **51:**1221–1232.
14. **Kappe, S. H., C. A. Buscaglia, and V. Nussenzweig.** 2004. *Plasmodium* sporozoite molecular cell biology. Annu. Rev. Cell Dev. Biol. **20:**29–59.
15. **Kappe, S. H., M. J. Gardner, S. M. Brown, J. Ross, K. Matuschewski, J. M. Ribeiro, J. H. Adams, J. Quackenbush, J. Cho, D. J. Carucci, S. L. Hoffman, and V. Nussenzweig.** 2001. Exploring the transcriptome of the malaria sporozoite stage. Proc. Natl. Acad. Sci. USA **98:**9895–9900.
16. **Kariu, T., T. Ishino, K. Yano, Y. Chinzei, and M. Yuda.** 2006. CelTOS, a novel malarial protein that mediates transmission to mosquito and vertebrate hosts. Mol. Microbiol. **59:**1369–1379.
17. **Ménard, R., and C. Janse.** 1997. Gene targeting in malaria parasites. Methods **13:**148–157.
18. **Menard, R., A. A. Sultan, C. Cortes, R. Altszuler, M. R. van Dijk, C. J. Janse, A. P. Waters, R. S. Nussenzweig, and V. Nussenzweig.** 1997. Circumsporozoite protein is required for development of malaria sporozoites in mosquitoes. Nature **385:**336–340.
19. **Mikolajczak, S. A., and S. H. Kappe.** 2006. A clash to conquer: the malaria parasite liver infection. Mol. Microbiol. **62:**1499–1506.
20. **Mota, M. M., G. Pradel, J. P. Vanderberg, J. C. Hafalla, U. Frevert, R. S. Nussenzweig, V. Nussenzweig, and A. Rodriguez.** 2001. Migration of *Plasmodium* sporozoites through cells before infection. Science **291:**141–144.
21. **Mueller, A. K., N. Camargo, K. Kaiser, C. Andorfer, U. Frevert, K. Matuschewski, and S. H. Kappe.** 2005. *Plasmodium* liver stage developmental arrest by depletion of a protein at the parasite-host interface. Proc. Natl. Acad. Sci. USA **102:**3022–3027.
22. **Mueller, A. K., M. Labaied, S. H. Kappe, and K. Matuschewski.** 2005. Genetically modified *Plasmodium* parasites as a protective experimental malaria vaccine. Nature **433:**164–167.
23. **Ponnudurai, T., A. H. Lensen, G. J. van Gemert, M. G. Bolmer, and J. H. Meuwissen.** 1991. Feeding behaviour and sporozoite ejection by infected *Anopheles stephensi*. Trans. R. Soc. Trop. Med. Hyg. **85:**175–180.
24. **Prudencio, M., A. Rodriguez, and M. M. Mota.** 2006. The silent path to thousands of merozoites: the *Plasmodium* liver stage. Nat. Rev. Microbiol. **4:**849–856.
25. **Quittnat, F., Y. Nishikawa, T. T. Stedman, D. R. Voelker, J. Y. Choi, M. M. Zahn, R. C. Murphy, R. M. Barkley, M. Pypaert, K. A. Joiner, and I. Coppens.** 2004. On the biogenesis of lipid bodies in ancient eukaryotes: synthesis of triacylglycerols by a *Toxoplasma* DGAT1-related enzyme. Mol. Biochem. Parasitol. **138:**107–122.
26. **Renia, L., A. C. Gruner, M. Mauduit, and G. Snounou.** 2006. Vaccination against malaria with live parasites. Expert Rev. Vaccines **5:**473–481.
27. **Renia, L., F. Miltgen, Y. Charoenvit, T. Ponnudurai, J. P. Verhave, W. E. Collins, and D. Mazier.** 1988. Malaria sporozoite penetration. A new approach by double staining. J. Immunol. Methods **112:**201–205.
28. **Silvie, O., C. Greco, J. F. Franetich, A. Dubart-Kupperschmitt, L. Hannoun, G. J. van Gemert, R. W. Sauerwein, S. Levy, C. Boucheix, E. Rubinstein, and D. Mazier.** 2006. Expression of human CD81 differently affects host cell susceptibility to malaria sporozoites depending on the *Plasmodium* species. Cell. Microbiol. **8:**1134–1146.
29. **Sultan, A. A., V. Thathy, U. Frevert, K. J. Robson, A. Crisanti, V. Nussenzweig, R. S. Nussenzweig, and R. Menard.** 1997. TRAP is necessary for gliding motility and infectivity of *plasmodium* sporozoites. Cell **90:**511–522.
30. **Tarun, A. S., R. F. Dumpit, N. Camargo, M. Labaied, P. Liu, A. Takagi, R. Wang, and S. H. Kappe.** 2007. Protracted sterile protection with *Plasmodium yoelii* pre-erythrocytic GAP malaria vaccines is independent of significant liver stage persistence and is mediated by CD8+ T cells. J. Infect. Dis., in press.
31. **Templeton, T. J., and D. C. Kaslow.** 1999. Identification of additional members define a *Plasmodium falciparum* gene superfamily which includes Pfs48/45 and Pfs230. Mol. Biochem. Parasitol. **101:**223–227.
32. **Tomas, A. M., G. Margos, G. Dimopoulos, L. H. van Lin, T. F. de Koning-Ward, R. Sinha, P. Lupetti, A. L. Beetsma, M. C. Rodriguez, M. Karras, A. Hager, J. Mendoza, G. A. Butcher, F. Kafatos, C. J. Janse, A. P. Waters, and R. E. Sinden.** 2001. P25 and P28 proteins of the malaria ookinete surface have multiple and partially redundant functions. EMBO J. **20:**3975–3983.
33. **Ungureanu, E., R. Killick-Kendrick, P. C. Garnham, P. Branzei, C. Romanescu, and P. G. Shute.** 1977. Prepatent periods of a tropical strain of *Plasmodium vivax* after inoculations of tenfold dilutions of sporozoites. Trans. R. Soc. Trop. Med. Hyg. **70:**482–483.

34. **Vanderberg, J. P., and U. Frevert.** 2004. Intravital microscopy demonstrating antibody-mediated immobilisation of *Plasmodium berghei* sporozoites injected into skin by mosquitoes. Int. J. Parasitol. **34:**991–996.
35. **van Dijk, M. R., B. Douradinha, B. Franke-Fayard, V. Heussler, M. W. van Dooren, B. van Schaijk, G. J. van Gemert, R. W. Sauerwein, M. M. Mota, A. P. Waters, and C. J. Janse.** 2005. Genetically attenuated, P36p-deficient malarial sporozoites induce protective immunity and apoptosis of infected liver cells. Proc. Natl. Acad. Sci. USA **102:**12194–12199.
36. **van Dijk, M. R., C. J. Janse, J. Thompson, A. P. Waters, J. A. Braks, H. J. Dodemont, H. G. Stunnenberg, G. J. van Gemert, R. W. Sauerwein, and W. Eling.** 2001. A central role for P48/45 in malaria parasite male gamete fertility. Cell **104:**153–164.

Editor: W. A. Petri, Jr.